Journal of chemical & engineering data

Article

pubs.acs.org/jced

# Aqueous Biphasic Systems Composed of Ionic Liquids and Acetate-Based Salts: Phase Diagrams, Densities, and Viscosities

Maria V. Quental,[†] Helena Passos,[†] Kiki A. Kurnia,[†,‡] João A. P. Coutinho,[†] and Mara G. Freire*[,†]

[†]CICECO —Aveiro Institute of Materials, Department of Chemistry, University of Aveiro, 3810-193 Aveiro, Portugal

[‡]Center of Research in Ionic Liquids, Department of Chemical Engineering, Universiti Teknologi PETRONAS, Tronoh 31750, Malaysia

Supporting Information

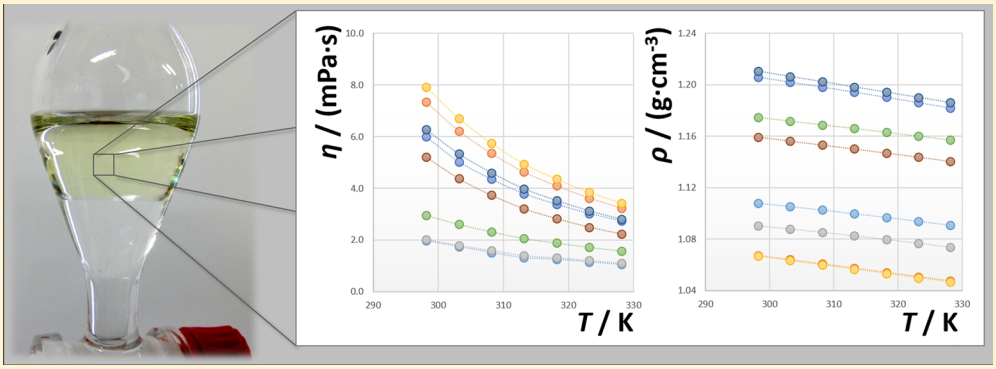


**ABSTRACT:** Ionic-liquid-based aqueous biphasic systems (IL-based ABS) have been largely investigated as promising extraction and purification routes. In this context, the determination of their phase diagrams and the physical properties of the coexisting phases are of high relevance when envisaging their large-scale applications. Low viscosities improve mass transfer and reduce energy consumption, while the knowledge of their densities is important for equipment design. In this work, novel phase diagrams for aqueous solutions of imidazolium-based ILs combined with acetate-based salts, namely $KCH_3CO_2$ or $NaCH_3CO_2$, are reported and discussed. The ability of the acetate-based salts to induce the phase separation not only depends on the ions hydration energy, but also on the concentration of "free" ions in solution. The tie-lines, tie-line lengths, and critical points are also addressed. Experimental measurements of density and viscosity of the coexisting phases, for the different systems and at several compositions and temperatures, are additionally presented. The Othmer–Tobias and Bancroft equations are also applied to ascertain the tie-lines coherence. It is here shown that low-viscous IL-based ABS, with a high difference in the densities of the coexisting phases, can be formed with organic and biodegradable salts thus offering enhanced features over conventional polymer-based systems.

## INTRODUCTION

Aqueous biphasic systems (ABS) have been investigated for the replacement of volatile and hazardous organic compounds in liquid–liquid extraction processes.[1−4] Typical ABS consist in two aqueous-rich phases containing polymer/polymer, polymer/salt or salt/salt combinations.[5] In the past decade, ionic-liquid-(IL)-based ABS appeared as a novel alternative to polymer-rich systems because of their enhanced performance in extraction and purification approaches.[5,6] In fact, the use of ILs as phase-forming components of ABS permits the tuning of the polarities and affinities of the coexisting phases and improved extractions and selectivities can be foreseen.[5]

Reliable thermophysical data of pure ILs and their mixtures are of paramount relevance to support their industrial applications.[7−10] These data are required in the development of models for process design, energy efficiency, and control of chemical processes.[7] In addition to the knowledge of the phase diagrams and compositions of the coexisting phases, the density and viscosity are also pertinent properties for the use of IL-based ABS at a large scale. Low viscosities of the coexisting phases enhance mass transfer and reduce energy consumption, while densities are important for equipment design. Although a large number of publications reporting the phase diagrams of IL-based ABS can be found,[5] few of them report the thermophysical properties of their coexisting phases.[11−14]

In literature, most works addressing IL-based ABS have considered high-charge density inorganic salts because of their strong salting-out character.[5] Nevertheless, the high concentrations of these salts required to form two-phase systems may have some adverse effects upon the (bio)molecules being purified and also lead to environmental concerns. Organic salts, known for their lower toxicity and favorable biodegradability,

**Received:** November 17, 2014
**Accepted:** April 28, 2015
**Published:** May 7, 2015

ACS Publications © 2015 American Chemical Society



DOI: 10.1021/je501044u
J. Chem. Eng. Data 2015, 60, 1674−1682

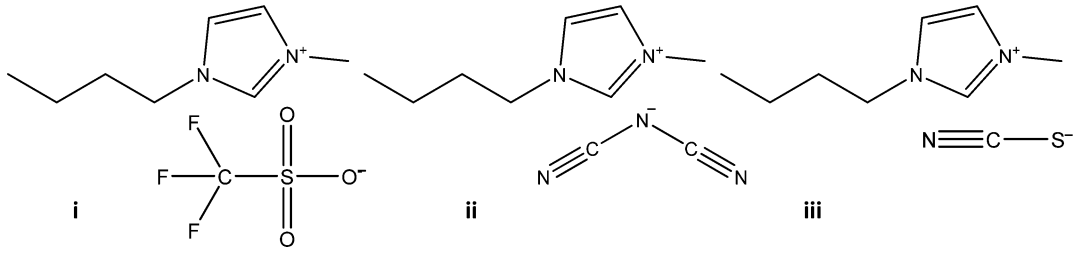


**Figure 1.** Chemical structure of the ILs studied: (i) $[C_4mim][CF_3SO_3]$, (ii) $[C_4mim][N(CN)_2]$, (iii) $[C_4mim][SCN]$.

can also form ABS when combined with ILs in aqueous solutions. Despite these advantages, few works on IL-based ABS formed by organic salts are available.[15−22] The ability of citrate-, tartrate-, and acetate-based salts to induce ABS with ILs has been reported.[15−22] However, acetate-based salts were only tested with $[BF_4]$-based ILs,[18−20] which are nonstable in water even at room temperature,[23] and with $[CF_3SO_3]$-based compounds.[20]

In this work, a set of imidazolium-based ILs with the ability to induce ABS formation when in the presence of sodium or potassium acetate salts, namely 1-butyl-3-methylimidazolium trifluoromethanesulfonate ($[C_4mim][CF_3SO_3]$), 1-butyl-3-methylimidazolium thiocyanate ($[C_4mim][SCN]$), and 1-butyl-3-methylimidazolium dicyanamide ($[C_4mim][N(CN)_2]$), were selected. The ternary phase diagrams at 298 K, as well as the respective tie-lines (TLs) and tie-line lengths (TLLs), were determined. As it will be shown, the ability of the acetate-based salts to induce the phase separation not only depends on their respective hydration energy, but also on the concentration of "free" ions in solution. In addition, the TLs were also validated using the Othmer−Tobias and Bancroft equations.[24,25] Finally, the physical properties of the coexisting phases, namely density and viscosity, were characterized to gather a broader picture on the applicability of these systems.

## EXPERIMENTAL SECTION

**Materials.** Potassium acetate, $KCH_3CO_2$, 99 wt % of purity from Sigma-Aldrich, and sodium acetate, $NaCH_3CO_2$, 99 wt % of purity from VWR, were used as received. Several imidazolium-based ILs, namely 1-butyl-3-methylimidazolium trifluoromethanesulfonate ($[C_4mim][CF_3SO_3]$), 1-butyl-3-methylimidazolium thiocyanate ($[C_4mim][SCN]$), and 1-butyl-3-methylimidazolium dicyanamide ($[C_4mim][N(CN)_2]$), acquired from Iolitec and with a purity level > 98 wt %, were investigated. The cation and anion chemical structures of the studied ILs are displayed in Figure 1. It should be highlighted that other ILs were investigated to form ABS with $KCH_3CO_2$ and $NaCH_3CO_2$, namely 1-butyl-3-methylimidazolium bromide ($[C_4mim]Br$), 1-butyl-3-methylimidazolium methylsulfate ($[C_4mim][CH_3SO_4]$), 1-butyl-3-methylimidazolium ethylsulfate ($[C_4mim][C_2H_5SO_4]$), 1-butyl-3-methylimidazolium tosylate ($[C_4mim][TOS]$), 1-butyl-3-methylimidazolium octylsulfate ($[C_4mim][C_8H_{17}SO_4]$), 1-hexyl-3-methylimidazolium chloride ($[C_6mim]Cl$), 1-methyl-3-octylimidazolium chloride ($[C_8mim]Cl$), 1-butyl-1-methylpiperidinium chloride ($[C_4mpip]Cl$), 1-butyl-1-methylpyrrolidinium chloride ($[C_4mpyr]Cl$), 1-butyl-3-metylpyridinium chloride ($[C_4mpy]Cl$), tetrabutylphosphonium chloride ($[P_{4444}]Cl$), tetrabutylammonium chloride ($[N_{4444}]Cl$), tributylmethylphosphonium tosylate ($[P_{4441}][TOS]$), tributylmethylphosphonium ethylsulfate ($[P_{4441}][C_2H_5SO_4]$), and tributylethylphosphonium diethylphosphate ($[P_{4442}][(C_2H_5)_2PO_2]$). Nevertheless, these ILs were not able to undergo liquid−liquid demixing with the acetate-based salts investigated. Before use, IL samples were purified and dried for a minimum of 24 h at constant agitation, at a moderate temperature (≈ 353 K), and under vacuum. After this step, the purity of each IL was further confirmed using $^1H$, $^{13}C$, and $^{19}F$ (whenever applicable) NMR spectroscopy. The water employed was ultrapure water, double distilled, and treated with a Milli-Q plus 185 water purification device.

**Phase Diagrams, Tie-Lines, Tie-Line Lengths and Critical Points.** The binodal curve of each ternary phase diagram was determined through the cloud point titration method at (298 ± 1) K and at atmospheric pressure. The experimental procedure adopted was validated by us in a previous work.[26] In brief, aqueous solutions of the acetate salts (≈ 25 wt %) and aqueous solutions of ILs with variable concentrations (from 60 wt % to 80 wt %) were prepared gravimetrically ($\pm 10^{-4}$ g) and used for the determination of the saturation curves. Drop-wise addition of the aqueous salt solution to each IL aqueous solution was carried out until the detection of a cloudy solution (biphasic region), followed by the dropwise addition of ultrapure water until the detection of a limpid solution (monophasic regime). In some situations, the addition of the IL solution to the salt-rich medium was also carried out to complete the phase diagrams. These additions were carried out under constant agitation. Each mixture composition was determined by the weight quantification of all components added within ± $10^{-4}$ g.

The tie-lines (TLs) of the system $[C_4mim][CF_3SO_3]$ + $NaCH_3CO_2$ were determined analytically (by quantifying the IL by UV spectroscopy, the water gravimetrically by evaporation down to a constant weight and the salt by weight difference), while the TLs of the systems $[C_4mim][SCN]$ + $NaCH_3CO_2$, $[C_4mim][CF_3SO_3]$ + $KCH_3CO_2$, $[C_4mim][SCN]$ + $KCH_3CO_2$ and $[C_4mim][N(CN)_2]$ + $KCH_3CO_2$ were determined by a gravimetric method originally described by Merchuk et al.[27] The method described by Merchuk et al.,[27] commonly applied to describe the binodal data of ABS, is not able to correctly describe TLs highly concentrated in IL and salt.[28] Some problems were found in the application of this method to the aqueous system formed by $[C_4mim][CF_3SO_3]$ and $NaCH_3CO_2$, where no consistency of the TLs' data was found, maybe due to the highly hydrophobicity of this IL which implies an IL-rich phase with a low water content. The selected mixture, at the biphasic regime, was prepared by weighting the appropriate amounts of salt + IL + water, vigorously stirred, and further submitted to centrifugation for 30 min and at controlled temperature, (298 ± 1) K. After centrifugation, each phase was carefully separated and weighed. For the first situation, the quantification of each compound in each phase was determined as described previously. For the gravimetric method approach, each individual TL was determined by the application of the lever-arm rule to the relationship between the weight of the top


DOI: 10.1021/je501044u
J. Chem. Eng. Data 2015, 60, 1674−1682

and bottom phases and the overall system composition. The experimental binodal curves were fitted using eq 1,[27]

$$100\ w_{IL} = A\ \exp[(B{\cdot}100\ w_{salt}{}^{0.5}) - (C{\cdot}100\ w_{salt}{}^{3})] \quad (1)$$

where 100 $w_{IL}$ and 100 $w_{salt}$ are the IL and salt weight fraction percentages, respectively, and $A$, $B$, and $C$ are fitted parameters obtained by least-squares regression.

For the determination of the TLs through the gravimetric approach, the following system of four equations (eqs 2 to 5) was used to estimate the composition of each phase (namely, 100 $w_{IL}^{IL}$, 100 $w_{salt}^{IL}$, 100 $w_{IL}^{salt}$ and 100 $w_{salt}^{salt}$):[27]

$$100\ w_{IL}^{IL} = A\ \exp[(B{\cdot}100\ w_{salt}^{IL\ 0.5}) - (C{\cdot}100\ w_{salt}^{IL\ 3})] \quad (2)$$

$$100\ w_{IL}^{salt} = A\ \exp[(B{\cdot}100\ w_{salt}^{salt\ 0.5}) - (C{\cdot}100\ w_{salt}^{salt\ 3})] \quad (3)$$

$$100\ w_{IL}^{IL} = \frac{100\ w_{IL}^{M}}{\alpha} - \frac{1-\alpha}{\alpha}{\cdot}100\ w_{IL}^{salt} \quad (4)$$

$$100\ w_{salt}^{IL} = \frac{100\ w_{salt}^{M}}{\alpha} - \frac{1-\alpha}{\alpha}{\cdot}100\ w_{salt}^{salt} \quad (5)$$

where the superscripts "IL" and "salt" designate the IL-rich and salt-rich aqueous phases, respectively, and "M" is the initial mixture composition. The parameter $\alpha$ is the ratio between the weight of the IL-rich phase and the total weight of the mixture. The solution of this system provides the concentration (wt %) of the salt and IL in the top and bottom phases. For the calculation of the tie-line lengths (TLLs), eq 6 was used,

$$TLL = \sqrt{(100\ w_{salt}^{IL} - 100\ w_{salt}^{salt})^2 + (100\ w_{IL}^{IL} - 100\ w_{IL}^{salt})^2} \quad (6)$$

The consistency of the measured TLs was further checked using the Othmer–Tobias[24]

$$\left(\frac{1-100\ w_{IL}^{IL}}{100\ w_{IL}^{IL}}\right) = k_1\left(\frac{1-100\ w_{salt}^{salt}}{100\ w_{salt}^{salt}}\right)^{n} \quad (7)$$

and Bancroft[25] equations,

$$\left(\frac{100\ w_{H_2O}^{salt}}{100\ w_{salt}^{salt}}\right) = k_2\left(\frac{100\ w_{H_2O}^{IL}}{100\ w_{IL}^{IL}}\right)^{r} \quad (8)$$

where $k_1$, $n$, $k_2$, and $r$ are fitting parameters. A linear dependency of log $((1-100\ w_{IL}^{IL})/(100\ w_{IL}^{IL}))$ against log $((1-100\ w_{salt}^{salt})/(100\ w_{salt}^{salt}))$ and log $((100\ w_{H_2O}^{salt})/(100\ w_{salt}^{salt}))$ against log $((100\ w_{H_2O}^{IL})/(100\ w_{IL}^{IL}))$ indicates the consistency of the results.

The critical point of each ABS was also determined by extrapolating the TLs' slopes of individual systems followed by the fitting using eq 9,

$$100\ w_{IL} = f100\ w_{salt} + g \quad (9)$$

where $f$ and $g$ are the fitting parameters.

**Ions Speciation.** The speciation of the salt ions in aqueous solution and the respective concentrations were estimated using VisualMINTEQ[29] (version 3.0), a thermodynamic speciation model, based on the MinteqA2 software with the Minteq database. Previously we confirmed the capability of Visual-MINTEQ to describe the metal salt ions speciation and its impact upon the formation of IL-based ABS.[20] In these thermodynamic calculations, the concentration of salt in each ternary mixture was used as the input.

**Density and Viscosity.** Density and viscosity measurements for both the IL-rich and organic-salt-rich phases were performed at atmospheric pressure and at the temperature range between (298.15 and 328.15) K, with an uncertainty of ± 0.02 K, using an automated SVM 3000 Anton Paar rotational Stabinger viscometer-densimeter. The dynamic viscosities have a relative uncertainty of 0.35 % while the absolute uncertainty for the density is $5 \times 10^{-4}$ g·cm$^{-3}$. Prior to the measurements, the equipment was calibrated using standard solutions, as well as with pure ILs or their mixtures.[7,30]

## RESULTS

**Phase Diagrams, Tie-Lines, Tie-Line Lengths and Critical Points.** Ternary phase diagrams were determined for each IL + $KCH_3CO_2$ + $H_2O$ (Figure 2) and IL + $NaCH_3CO_2$ + $H_2O$ (Figure 3) system, at 298 K and at atmospheric pressure. To form ABS, that is, two aqueous rich-phases, composed of ILs and salts, only hydrophilic or water-miscible ILs should be chosen. Among all the studied ILs, only [$C_4$mim][$CF_3SO_3$], [$C_4$mim][SCN], and [$C_4$mim][$N(CN)_2$] were able to promote

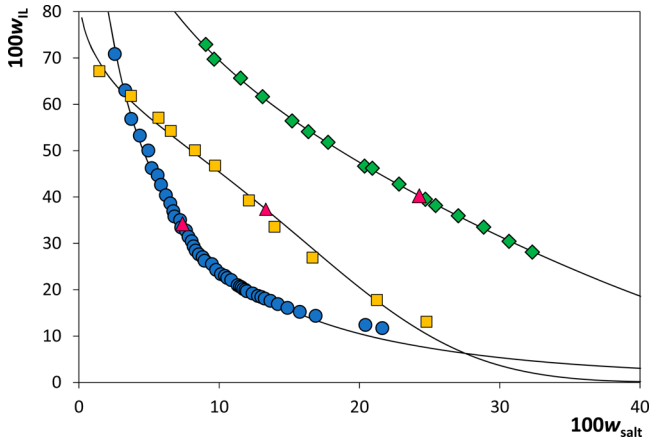


**Figure 2.** Ternary phase diagrams for ABS composed of IL + $KCH_3CO_2$ + $H_2O$: [$C_4$mim][$CF_3SO_3$] (blue ●); [$C_4$mim][SCN] (yellow ■); [$C_4$mim][$N(CN)_2$] (green ◆); critical point (red ▲); adjusted binodal using eq 1 (−).

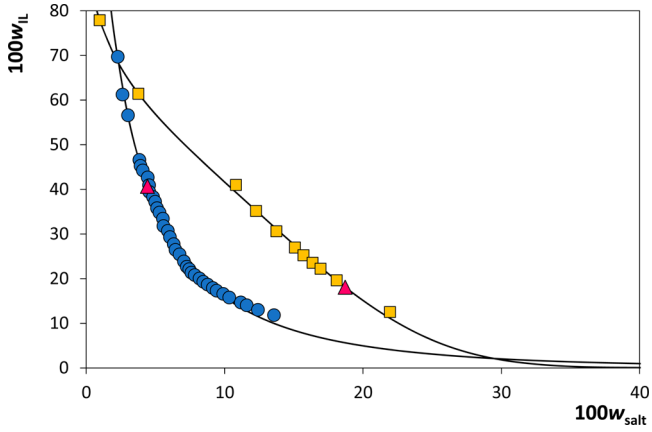


**Figure 3.** Ternary phase diagrams for ABS composed of IL + $NaCH_3CO_2$ + $H_2O$: [$C_4$mim][$CF_3SO_3$] (blue ●); [$C_4$mim][SCN] (yellow ■); critical point (red ▲); adjusted binodal using eq 1 (−).



DOI: 10.1021/je501044u
J. Chem. Eng. Data 2015, 60, 1674−1682

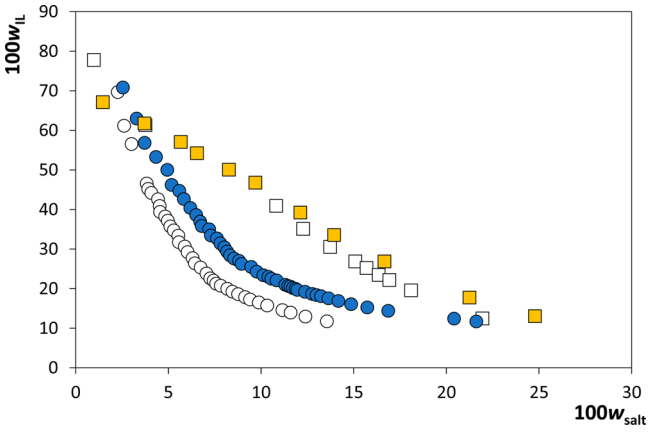


**Figure 4.** Evaluation of salt effect on the formation of [$C_4$mim]-[$CF_3SO_3$]- (blue ●) and [$C_4$mim][SCN]-based ABS (yellow ■): $KCH_3CO_2$ (full symbols) and $NaCH_3CO_2$ (open symbols).

the ABS formation with acetate-based salts. These ILs comprise imidazolium-based cations with a butyl chain that turns the IL more hydrophobic that makes them more easily undergo phase-separation, and anions with a low hydrogen-bond basicity or a weak ability to accept protons from water.[31] For most systems, the top phase corresponds to the IL-rich phase while the bottom phase represents the salt-rich phase. An exception was observed for the ABS containing [$C_4$mim][$CF_3SO_3$]. The phase inversion is directly related to the high density of the fluorinated anion.[32]

In Figures 2 and 3, the biphasic regime is located above the solubility curve. The area of this region is proportional to the ability of each IL to undergo liquid−liquid demixing with salt solutions. The aptitude of each IL to form two phases in the presence of ∼10 wt % of $KCH_3CO_2$ is as follows: [$C_4$mim]-[$CF_3SO_3$] > [$C_4$mim][SCN] > [$C_4$mim][$N(CN)_2$]. This rank to promote phase separation is similar to previous results for ABS composed of ILs and $NaSO_4$,[33] citrate-based[22] and phosphate-based[26] salts. Previous works[34−36] have shown that water mainly interacts with ILs through its anion, in which it plays a major role as a hydrogen-bond acceptor. Furthermore, the ability of the IL anions to form ABS closely follows the decrease on their hydrogen-bond accepting strength or electron pair donation ability.[26] The same trend of ILs to promote ABS was observed for ∼10 wt % of $NaCH_3CO_2$; however, it is interesting to highlight that this salt is not able to form ABS with [$C_4$mim][$N(CN)_2$], despite its higher hydration energy ($\Delta G_{hyd}$ ($Na^+$) = −365 kJ·mol$^{-1}$ and $\Delta G_{hyd}$ ($K^+$) = −295 kJ·mol$^{-1}$).[21,37]

The formation of ABS with ILs and salts is normally characterized by the occurrence of a competition between the IL and salt ions to be solvated by water. The competition is won by the salt ions due to their higher hydration energy when compared to IL ions. Consequently, there is a migration of water from the IL-solvated region toward the salt-rich phase and thus forming two liquid phases. The strength of the salt ions to be solvated by water can be characterized either by the Gibbs free energy ($\Delta G_{hyd}$) or the molar entropy of hydration ($\Delta S_{hyd}$). The lower $\Delta G_{hyd}$ and $\Delta S_{hyd}$ of the acetate ion when compared with other high-charge density anions, for instance $PO_4^{3-}$,[26,38] confirms its weaker salting-out ability (according to the Hofmeister series[21,39]) and, consequently, a lower aptitude to create ABS with ILs.

As the studied salts share the same anion, the capability of the salts to promote ABS depends on their cation counterpart, $Na^+$ and $K^+$. Figure 4 depicts the effect of the salt on the formation of two-phase systems. $NaCH_3CO_2$ is more able to form ABS, that is, lower amounts of salt are required for the liquid−liquid demixing. This trend is in agreement with the $\Delta G_{hyd}$ and $\Delta S_{hyd}$ of the respective salt cations: $Na^+$ ($\Delta G_{hyd}$ = −365 kJ·mol$^{-1}$, $\Delta S_{hyd}$ = −111 J·K$^{-1}$·mol$^{-1}$) and $K^+$ ($\Delta G_{hyd}$ = −295 kJ·mol$^{-1}$, $\Delta S_{hyd}$ = −74 J·K$^{-1}$·mol$^{-1}$).[21,37] Thus, if $KCH_3CO_2$ can form ABS with [$C_4$mim][$N(CN)_2$], one might also expect that $NaCH_3CO_2$, with higher $\Delta G_{hyd}$ and $\Delta S_{hyd}$, should also form ABS. Nevertheless, the unexpected inability of $NaCH_3CO_2$ to promote phase separation with aqueous solutions of [$C_4$mim][$N(CN)_2$] is an indication that the formation of ABS is not only governed by the Gibbs free energy of hydration (or molar entropy of hydration). In fact, the concentration of "free" ions in aqueous solution plays a major role as discussed below.

Several works[37,40−42] have addressed the presence of ion pairs of organic (or inorganic) salts in aqueous solution. For instance, using Raman spectroscopy, Fournier and co-workers[42] confirmed ion pairing of $NaCH_3CO_2$ in aqueous media. In a previous work,[20] we have shown that the ion pairing of polyvalent salt ions has a significant impact toward their ability to promote phase separation in ABS. Therefore, we turned here our attention to estimate the ions speciation that might occur in aqueous solutions of $NaCH_3CO_2$ and $KCH_3CO_2$ with an aim to understand the inability of the sodium-based salt to form ABS with [$C_4$mim][$N(CN)_2$]. Details on the speciation of the ions, at 298 K, along with their concentration are given in the Supporting Information. It is shown that, for the concentration range where the salt is able to form ABS, the dissolution of $NaCH_3CO_2$ in aqueous media produces not only $Na^+$ and $CH_3CO_2^-$ but also $NaCH_3CO_2$. In addition, the concentration of the $NaCH_3CO_2$ ion pair increases with an increase in the concentration of salt. Although a similar trend is observed for the dissolution of $KCH_3CO_2$, in which it produces the $KCH_3CO_2$ ion pair, when comparing the ion speciation profiles of both salts, it is interesting to note that for the same concentration, the sodium-based salt presents a higher abundance of the pair $NaCH_3CO_2$. This ion pairing reduces therefore the concentration of "free" and further hydrated $Na^+$

**Table 1. Correlation Parameters Used to Describe the Experimental Binodal Data by eq 1 and Respective Standard Deviations ($\sigma$) and Correlation Coefficients ($R^2$)**

| IL | salt | $A \pm \sigma$ | $B \pm \sigma$ | $10^5$ ($C \pm \sigma$) | $R^2$ |
|---|---|---|---|---|---|
| [$C_4$mim][$CF_3SO_3$] | $KCH_3CO_2$ | 209.0 ± 1.8 | −0.67 ± 0.03 | 0.01 ± 0.19 | 0.998 |
| [$C_4$mim][SCN] | | 84.9 ± 3.7 | −0.17 ± 0.02 | 18.14 ± 0.95 | 0.992 |
| [$C_4$mim][$N(CN)_2$] | | 205.8 ± 13.9 | −0.57 ± 0.02 | 1.00 ± 0.43 | 0.996 |
| [$C_4$mim][$CF_3SO_3$] | $NaCH_3CO_2$ | 265.1 ± 9.7 | −0.89 ± 0.02 | 0.01 ± 3.20 | 0.995 |
| [$C_4$mim][SCN] | | 98.9 ± 1.8 | −0.24 ± 0.01 | 9.94 ± 0.70 | 0.999 |



DOI: 10.1021/je501044u
J. Chem. Eng. Data 2015, 60, 1674−1682

**Table 2. Weight Fraction Compositions (100 $w$) for TLs and Respective TLLs of IL + $KCH_3CO_2$ + $H_2O$ and IL + $NaCH_3CO_2$ + $H_2O$ ABS, at the Top (T) and Bottom (B) Phases and at the Initial Biphasic Composition of the Mixture (M) at 298 K and at Atmospheric Pressure (0.1 MPa). Viscosity and Density Properties Were Measured for the Identified TLs (ID)[a]**

| | | weight fraction composition/wt % | | | | | | | | | | |
|---|---|---|---|---|---|---|---|---|---|---|---|---|
| IL | salt | 100 $w^T_{IL}$ | 100 $w^T_{salt}$ | 100 $w^T_{water}$ | 100 $w^M_{IL}$ | 100 $w^M_{salt}$ | 100 $w^M_{water}$ | 100 $w^B_{IL}$ | 100 $w^B_{salt}$ | 100 $w^B_{water}$ | TLL | ID |
| $[C_4mim][CF_3SO_3]$ | $KCH_3CO_2$ | 18.31 | 13.23 | 68.46 | 24.22 | 11.83 | 63.95 | 57.41 | 3.74 | 38.85 | 47.76 | TL1 |
| | | 11.83 | 18.47 | 69.70 | 25.95 | 15.07 | 58.98 | 80.16 | 2.06 | 17.78 | 70.27 | |
| | | 10.67 | 19.80 | 69.53 | 29.88 | 15.11 | 55.01 | 84.15 | 1.85 | 14.00 | 75.63 | |
| $[C_4mim][SCN]$ | | 64.76 | 2.46 | 32.78 | 40.18 | 13.81 | 46.01 | 2.83 | 31.07 | 66.10 | 68.22 | TL1 |
| | | 81.31 | 0.06 | 18.63 | 40.13 | 19.84 | 40.03 | 0.23 | 38.99 | 60.78 | 89.93 | TL2 |
| | | 82.76 | 0.02 | 17.22 | 39.94 | 22.23 | 37.83 | 0.04 | 42.93 | 57.03 | 93.18 | |
| $[C_4mim][N(CN)_2]$ | | 63.57 | 12.23 | 24.20 | 39.84 | 26.91 | 33.25 | 18.51 | 40.11 | 41.38 | 52.99 | |
| | | 71.70 | 9.25 | 19.05 | 39.97 | 28.94 | 31.09 | 12.55 | 45.94 | 41.51 | 69.60 | |
| | | 75.10 | 8.18 | 16.72 | 41.18 | 28.88 | 29.94 | 11.78 | 46.81 | 41.41 | 74.18 | |
| | | 76.41 | 7.80 | 15.79 | 39.86 | 30.93 | 29.21 | 8.71 | 50.65 | 40.64 | 80.12 | TL1 |
| | | 84.27 | 5.77 | 9.96 | 39.88 | 32.96 | 27.16 | 7.06 | 53.06 | 39.88 | 90.53 | TL2 |
| $[C_4mim][CF_3SO_3]$ | $NaCH_3CO_2$ | 6.61 | 17.69 | 75.70 | 29.82 | 11.70 | 58.48 | 73.56 | 2.20 | 24.24 | 68.72 | |
| | | 5.40 | 19.94 | 74.66 | 29.99 | 14.06 | 55.95 | 79.56 | 2.04 | 18.40 | 76.23 | |
| | | 5.32 | 21.20 | 73.48 | 30.08 | 15.54 | 54.38 | 82.22 | 2.24 | 15.54 | 79.22 | TL1 |
| $[C_4mim][SCN]$ | | 60.68 | 3.97 | 35.35 | 33.60 | 15.12 | 51.23 | 3.86 | 27.11 | 69.03 | 61.34 | TL1 |
| | | 82.93 | 0.53 | 16.54 | 33.02 | 18.86 | 48.12 | 1.59 | 30.41 | 68.00 | 86.65 | TL2 |
| | | 88.65 | 0.20 | 11.15 | 33.58 | 20.69 | 45.73 | 0.80 | 32.58 | 66.62 | 93.36 | |

[a]The standard uncertainty for the weight fraction $u(100\ w)$ is 0.01, the standard uncertainty for the temperature $u(T)$ is 1 K, and the standard uncertainty for pressure $u(P)$ is 10 kPa.

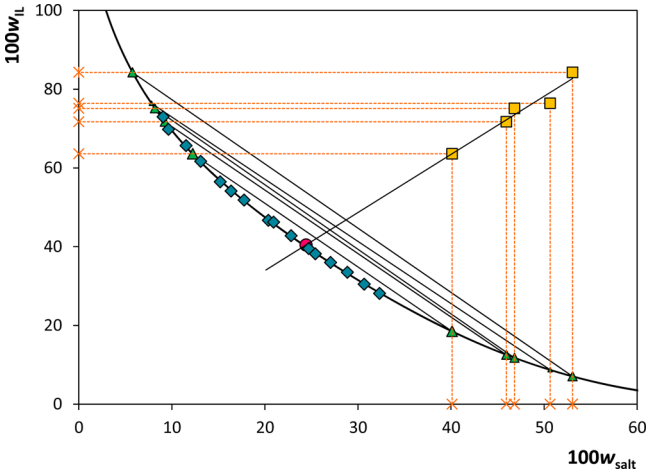


**Figure 5.** Phase diagram for the ternary system composed of $[C_4mim][N(CN)_2]$ + $KCH_3CO_2$ + $H_2O$: binodal curve data (blue ◆); adjusted binodal data through eq 1 (−); TL data (green ▲); TLs relation (yellow ■); critical point (red ●).

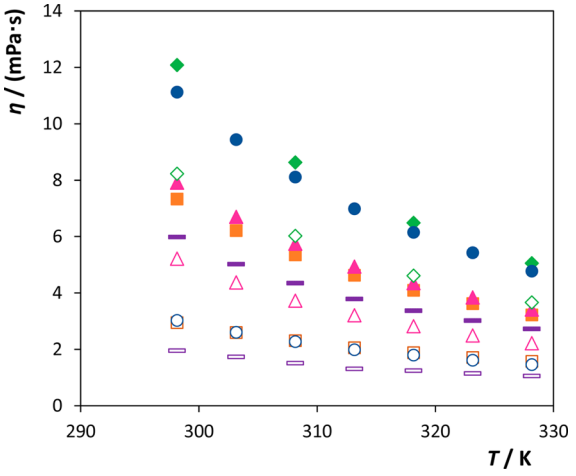


**Figure 6.** Experimental viscosity as a function of temperature for IL-rich (full symbols) and salt-rich (open symbols) phases of ternary mixtures identified in Table 2 as TL1: $[C_4mim][CF_3SO_3]$ + $KCH_3CO_2$ (−); $[C_4mim][CF_3SO_3]$ + $NaCH_3CO_2$ (blue ●); $[C_4mim][SCN]$ + $KCH_3CO_2$ (orange ■); $[C_4mim][SCN]$ + $NaCH_3CO_2$ (red ▲); $[C_4mim][N(CN)_2]$ + $KCH_3CO_2$ (green ◆).

and $CH_3CO_2^-$, that coupled with the weaker ability of $[C_4mim][N(CN)_2]$ to form ABS, support the inexistence of a two-phase system for the $NaCH_3CO_2$/$[C_4mim][N(CN)_2]$ combination.

The parameters obtained by the regression of the experimental binodal curves using eq 1 are presented in

**Table 3. Values of the Fitting Parameters of eqs 7 and 8 for the Systems Composed of IL+ Salt + $H_2O$ at 298 K, and Respective Standard Deviations ($\sigma$) and Correlation Coefficients ($R^2$)**

| | | Othmer–Tobias[24] (eq 7) | | | Bancrof[25] (eq 8) | | |
|---|---|---|---|---|---|---|---|
| IL | salt | $n \pm \sigma$ | $k_1 \pm \sigma$ | $R^2$ | $r \pm \sigma$ | $k_2 \pm \sigma$ | $R^2$ |
| $[C_4mim][CF_3SO_3]$ | $KCH_3CO_2$ | 2.846 ± 0.051 | 0.004 ± 0.036 | 1.000 | 0.275 ± 0.004 | 5.734 ± 0.003 | 1.000 |
| $[C_4mim][SCN]$ | | 1.970 ± 0.445 | 0.109 ± 0.107 | 0.951 | 0.477 ± 0.117 | 2.962 ± 0.066 | 0.943 |
| $[C_4mim][N(CN)_2]$ | | 1.945 ± 0.344 | 0.273 ± 0.030 | 0.914 | 0.271 ± 0.049 | 1.307 ± 0.021 | 0.910 |
| $[C_4mim][CF_3SO_3]$ | $NaCH_3CO_2$ | 2.264 ± 0.011 | 0.011 ± 0.007 | 1.000 | 0.379 ± 0.001 | 6.518 ± 0.001 | 1.000 |
| $[C_4mim][SCN]$ | | 6.285 ± 0.645 | 0.001 ± 0.240 | 0.990 | 0.138 ± 0.017 | 2.751 ± 0.011 | 0.985 |



DOI: 10.1021/je501044u
J. Chem. Eng. Data 2015, 60, 1674−1682

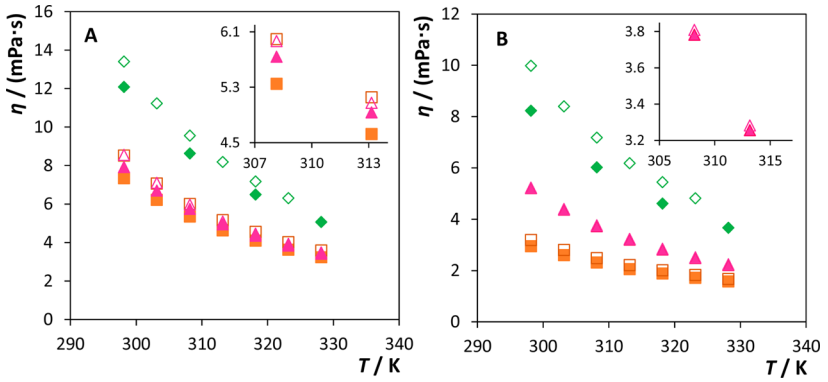


**Figure 7.** Experimental viscosity as a function of temperature for ternary mixtures identified in Table 2 as TL1 (full symbols) and TL2 (open symbols): $[C_4mim][SCN] + KCH_3CO_2$ (orange ■); $[C_4mim][SCN] + NaCH_3CO_2$ (red ▲); $[C_4mim][N(CN)_2] + KCH_3CO_2$ (green ◆). A, IL-rich phase; B, salt-rich phase.

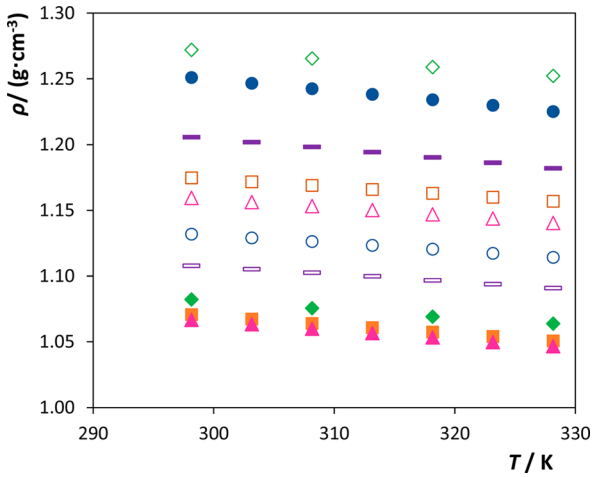


**Figure 8.** Experimental density as a function of temperature for IL-rich (full symbols) and salt-rich (open symbols) phases of ternary mixtures identified in Table 2 as TL1: $[C_4mim][CF_3SO_3] + KCH_3CO_2$ (−) $[C_4mim][CF_3SO_3] + NaCH_3CO_2$ (blue ●); $[C_4mim][SCN] + KCH_3CO_2$ (orange ■); $[C_4mim][SCN] + NaCH_3CO_2$ (red ▲); $[C_4mim][N(CN)_2] + KCH_3CO_2$ (green ◆).

Table 1. In general, good correlation coefficients were obtained for all systems, indicating that these fittings can be used to predict data in a given region of the phase diagram where no experimental results are offered. The detailed experimental weight fraction data for each phase diagram are reported in the Supporting Information.

The experimental TLs, along with their respective length (TLL), are reported in Table 2. Their representation can be found in the Supporting Information. In addition, the critical point of each system was also determined using eq 9 based on a geometrical approach schematized in Figure 5 for the system composed of $[C_4mim][N(CN)_2] + KCH_3CO_2 + H_2O$. The critical points of all the investigated systems are depicted in Figures 2 and 3. For the potassium-based ABS, the content of IL at the critical point is similar among all the systems investigated, while a larger difference is noticeable in the salt amount. On the other hand, for the stronger salting-out salt, $NaCH_3CO_2$, the critical point is more dependent on the type and amount of IL and salt.

The consistency of the TLs was further checked using the Othmer−Tobias[24] and Bancroft[25] equations (eqs 7 and 8), and the respective fitting parameters and correlation coefficient ($R^2$) are shown in Table 3 (cf. the Supporting Information with the graphical representation). The TL data are reliable since the obtained regression coefficients are close to 1, indicating therefore a good degree of consistency of the experimental data.

**Density and Viscosity.** The characterization of the top and bottom phases in different ternary systems, at different compositions and temperatures, are important for the design and scale up of extraction processes. Hence, the density and viscosity in the temperature range between 298.15 K and 328.15 K were determined for one or two ternary compositions

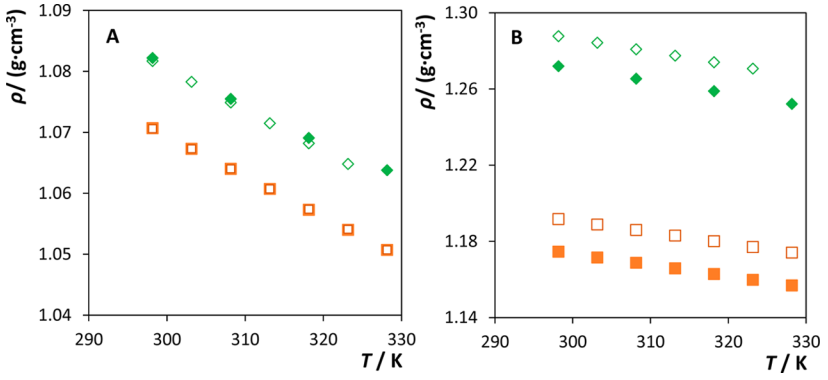


**Figure 9.** Experimental density as a function of temperature for ternary mixtures identified in Table 2 as TL1 (full symbols) and TL2 (open symbols): $[C_4mim][SCN] + KCH_3CO_2$ (orange ■); $[C_4mim][N(CN)_2] + KCH_3CO_2$ (green ◆). A, IL-rich phase; B, salt-rich phase.



DOI: 10.1021/je501044u
J. Chem. Eng. Data 2015, 60, 1674−1682

of each ABS studied. The following mixture compositions were investigated: 12 wt % of $KCH_3CO_2$ + 24 wt % of $[C_4mim][CF_3SO_3]$ + 64 wt % of $H_2O$ (TL1); 31 wt % of $KCH_3CO_2$ + 40 wt % of $[C_4mim][N(CN_2)]$ + 29 wt % of $H_2O$ (TL1); 33 wt % of $KCH_3CO_2$ + 40 wt % of $[C_4mim][N(CN_2)]$ + 27 wt % of $H_2O$ (TL2); 14 wt % of $KCH_3CO_2$ + 40 wt % $[C_4mim][SCN]$ + 46 wt % of $H_2O$ (TL1); 20 wt % of $KCH_3CO_2$ + 40 wt % $[C_4mim][SCN]$ + 40 wt % of $H_2O$ (TL2); 15 wt % of $NaCH_3CO_2$ + 30 wt % $[C_4mim][CF_3SO_3]$ + 64 wt % of $H_2O$ (TL1); 15 wt % of $NaCH_3CO_2$ + 34 wt % of $[C_4mim][SCN]$ + 51 wt % of $H_2O$ (TL1); 19 wt % of $NaCH_3CO_2$ + 33 wt % of $[C_4mim][SCN]$ + 29 wt % of $H_2O$ (TL2) (cf. Table 2 with the respective TLs data). Figures 6 to 9 show the density and viscosity data, as a function of temperature, for the mixtures investigated. The complete experimental data are available in the Supporting Information.

Viscosity is mainly dependent on intra- and intermolecular interactions. Since aqueous solutions of ILs and salts are being analyzed, H-bonding and Coulombic interactions are among the most important. An increase in temperature substantially decreases the intensity of H-bonding interactions and, therefore, the viscosity decreases with an increase in temperature, as shown in Figures 6 and 7.

Figure 6 displays the IL anion effect on the viscosity of the IL-rich and salt-rich phases for ABS composed of $KCH_3CO_2$ and $NaCH_3CO_2$. At 298.15 K and at the TL1′ compositions (Table 2), the viscosity of the IL-rich phase of the $KCH_3CO_2$-based ABS decreases in the following order: $[C_4mim][N(CN)_2]$ (12.08 mPa·s) > $[C_4mim][SCN]$ (7.33 mPa·s) > $[C_4mim][CF_3SO_3]$ (5.99 mPa·s). The opposite trend was observed with $NaCH_3CO_2$ where the viscosity decreases in the rank: $[C_4mim][CF_3SO_3]$ (11.12 mPa·s) > $[C_4mim][SCN]$ (7.91 mPa·s). For the salt-rich phase of ABS composed of $KCH_3CO_2$ the trend observed was as follows: $[C_4mim][N(CN)_2]$ (8.23 mPa·s) > $[C_4mim][SCN]$ (2.95 mPa·s) > $[C_4mim][CF_3SO_3]$ (1.96 mPa·s); for $NaCH_3CO_2$-based ABS the series is as follows: $[C_4mim][SCN]$ (5.21 mPa·s) > $[C_4mim][CF_3SO_3]$ (3.03 mPa·s). In general, the trend on the viscosity values of both phases seems to be closely related with their compositions. For IL-rich phases, the viscosity decreases with a decrease in the IL content and concomitant increase in the water amount (data given in Table 2). For $KCH_3CO_2$-based ABS at 298 K, the viscosity decreases in the order $[C_4mim][N(CN)_2]$ (76.41 wt % of IL, 15.79 wt % of $H_2O$) > $[C_4mim][SCN]$ (64.76 wt % of IL, 32.78 wt % of $H_2O$) > $[C_4mim][CF_3SO_3]$ (57.41 wt % of IL, 38.85 wt % of $H_2O$); and for $NaCH_3CO_2$-based ABS at 298 K: $[C_4mim][CF_3SO_3]$ (82.22 wt % of IL, 15.54 wt % of $H_2O$) > $[C_4mim][SCN]$ (60.68 wt % of IL, 35.35 wt % of $H_2O$). In a similar way, the viscosity of the salt-rich phase decreases with the increase on the water content and simultaneous decrease on the salt content according to the rank $[C_4mim][N(CN)_2]$ (50.65 wt % of salt, 40.64 wt % of water) > $[C_4mim][SCN]$ (31.07 wt % of salt, 66.10 wt % of water) > $[C_4mim][CF_3SO_3]$ (13.23 wt % of salt, 68.46 wt % of water) for $KCH_3CO_2$-based ABS, and $[C_4mim][SCN]$ (27.11 wt % of salt, 69.03 wt % of water) > $[C_4mim][CF_3SO_3]$ (21.20 wt % of salt, 73.48 wt % of water) for $NaCH_3CO_2$-based ABS.

Different ABS compositions were also investigated, and from the results displayed in Figure 7, the viscosities differences among the coexisting phases generally increase with the increase of the TLL (from TL1 to TL2) due to the larger differences in the mixture compositions (*cf.* Table 2).

Comparing the viscosity values obtained for $KCH_3CO_2$ + $[C_4mim][SCN]$ and $NaCH_3CO_2$ + $[C_4mim][SCN]$ ABS (Figure 6 and 7), it seems that the type of salt used in the ABS formulation does not influence the viscosity of the IL-rich phases—probably due to their low concentration in these phases (less than 4 wt %). On the other hand, salt-rich phases are composed of ca. 30 wt % of each salt, and there are significant differences in the viscosity values of these phases that are further dependent on the salt used in the preparation of a given ABS.

One of the critical problems related with conventional ABS composed of polymers is the high viscosity of the polymeric-rich phase which hinders the mass transfer and adds significant energetic inputs into the process.[43] It was already demonstrated that phosphonium-$K_3PO_4$-based ABS display lower viscosities than polymer-based ABS.[12] In addition, a recent work comprising ABS composed of imidazolium-based ILs and $K_3PO_4$ reported that imidazolium-based ABS lead to coexisting phases of lower viscosity than their phosphonium counterparts.[11] In general, while the viscosities of the IL-rich phases here studied are 1.5 to 3 times higher than those of the salt-rich ones, these are of a much lower viscosity than those of typical polymer-based ABS.[44]

Density data for all the studied systems are presented in Figures 8 and 9. In general, the density decreases with the increase of temperature. For most systems, and for both salts, the density of the salt-rich phase is higher than the density of the IL-rich phase. An exception was observed with the $[C_4mim][CF_3SO_3]$-based ABS—the IL-rich phase presents a higher density than the salt-rich phase (Figure 8). This is a consequence of the low concentration of inorganic salt at the IL-rich phase and of the high density of the fluorinated IL.

For the ABS formed by $KCH_3CO_2$, the density values of the IL-rich phases at 298.15 K and at the TL1′ compositions, are 1.0707 $g \cdot cm^{-3}$ for $[C_4mim][SCN]$, 1.0822 $g \cdot cm^{-3}$ for $[C_4mim][N(CN)_2]$, and 1.2058 $g \cdot cm^{-3}$ for $[C_4mim][CF_3SO_3]$. For ABS composed of $[C_4mim][SCN]$ + $NaCH_3CO_2$ and $[C_4mim][CF_3SO_3]$ + $NaCH_3CO_2$ the densities of the IL-rich phases are 1.0667 $g \cdot cm^{-3}$ and 1.2509 $g \cdot cm^{-3}$, respectively. These tendencies are in close agreement with other systems previously reported.[11,13] Moreover, when compared with other salts, such as $K_3PO_4$, the densities of the IL-rich phases are quite similar; for instance, at 298.15 K, the densities range between 1.2169 $g \cdot cm^{-3}$ ($[C_4mim][CF_3SO_3]$) and 1.0366 $g \cdot cm^{-3}$ ($[C_4mim][N(CN)_2]$).[11]

For salt-rich phases the density values at 298.15 K for both the studied salts are very similar: 1.1746 $g \cdot cm^{-3}$ for $[C_4mim][SCN]$ + $KCH_3CO_2$ (TL1) and 1.1594 $g \cdot cm^{-3}$ for $[C_4mim][SCN]$ + $NaCH_3CO_2$ (TL1). These results indicate that the change of the cation of the salt does not induce considerable variations in the densities of the coexisting phases. Nevertheless, the differences between the IL-rich and salt-rich phases cannot be neglected (Figure 8). As observed for viscosity, the density differences between the phases increase with the TLL (from TL1 to TL2 - Figure 9 and Table 2). For the IL-rich phase the density values are very close for the two TLLs tested (they are overlapped). On the other hand, for the salt-rich phase, an increase in the TLL leads to an increase in the density values as presented in Figure 9. In fact, for TL2, the amount of salt at the salt-rich phase is higher (shown in Table 2).

Compared with that of typical polymer−salt ABS,[45] the differences in the densities of the coexisting phases are higher for IL-based ABS. This is a very relevant result since higher


DOI: 10.1021/je501044u
J. Chem. Eng. Data 2015, 60, 1674−1682

density differences allow an easier and faster separation of the coexisting phases in ABS.

## CONCLUSIONS

ILs are currently seen as potential phase-forming promoters of ABS to be used in liquid−liquid separation processes. With a goal to develop more benign systems, we report here novel ternary phase diagrams, TLs, TLLs, and critical points for ABS composed of imidazolium-based ILs and two biodegradable organic salts (potassium and sodium acetate). It was found that the phase-separation ability of the investigated ILs follows the order $[C_4mim][CF_3SO_3]$ > $[C_4mim][SCN]$ > $[C_4mim][N(CN)_2]$. Sodium acetate revealed to be a stronger salting-out agent or having a higher capacity to form ABS. Furthermore, the coherence of the TL data were ascertained using the Othmer−Tobias and Bancroft equations. The densities and viscosities of the coexisting phases at given mixtures of all IL-based ABS were also determined. The system formed by $KCH_3CO_2$ and $[C_4mim][CF_3SO_3]$ presents the lower viscosity values, while the system constituted by $KCH_3CO_2$ + $[C_4mim][N(CN)_2]$ is the most viscous. Nevertheless, the viscosities of the coexisting phase of the investigated IL-based ABS were found to be substantially lower than those observed in typical polymer-based systems, representing thus a major contribution for the development of industrial processes based on ILs. At last, it was observed that the differences in the densities of the coexisting phases are higher for IL-based ABS than for polymer-based systems, allowing therefore an easier and faster separation of the coexisting phases.

## ASSOCIATED CONTENT

### Supporting Information

Binodal curves, ions speciation profiles, experimental data of density, and viscosity dependence with temperature and Othmer−Tobias and Bancroft correlations. The Supporting Information is available free of charge on the ACS Publications website at DOI: 10.1021/je501044u.

## AUTHOR INFORMATION

### Corresponding Author

*Tel: +351-234-401422. Fax: +351-234-370084. E-mail: maragfreire@ua.pt.

### Funding

This work was developed in the scope of the project CICECO-Aveiro Institute of Materials (ref. FCT UID/CTM/50011/2013), financed by national funds through the FCT/MEC and when applicable cofinanced by FEDER under the PT2020 Partnership. K. A. Kurnia and H. Passos acknowledge FCT for the postdoctoral and doctoral grants, SFRH/BPD/88101/2012 and SFRH/BD/85248/2012, respectively. M. G. Freire acknowledges the European Research Council (ERC) for the Starting Grant ERC-2013-StG-337753.

### Notes

The authors declare no competing financial interest.

## REFERENCES

(1) Albertsson, P. A. *Partitioning of Cell Particles and Macromolecules*; Wiley-Interscience: New York, 1986.

(2) Merchuk, J. C.; Andrews, B. A.; Asenjo, J. A. Aqueous two-phase systems for protein separation: Studies on phase inversion. *J. Chromatogr. B Biomed. Sci. Appl.* **1998**, *711*, 285−293.

(3) Hatti-Kaul, R. Aqueous two-phase systems. *Mol. Biotechnol.* **2001**, *19*, 269−277.

(4) Johansson, H.-O.; Karlström, G.; Tjerneld, F.; Haynes, C. A. Driving forces for phase separation and partitioning in aqueous two-phase systems. *J. Chromatogr. B Biomed. Sci. Appl.* **1998**, *711*, 3−17.

(5) Freire, M. G.; Cláudio, A. F. M.; Araújo, J. M. M.; Coutinho, J. A. P.; Marrucho, I. M.; Canongia Lopes, J. N.; Rebelo, L. P. N. Aqueous biphasic systems: A boost brought about by using ionic liquids. *Chem. Soc. Rev.* **2012**, *41*, 4966−4995.

(6) Gutowski, K. E.; Broker, G. A.; Willauer, H. D.; Huddleston, J. G.; Swatloski, R. P.; Holbrey, J. D.; Rogers, R. D. Controlling the aqueous miscibility of ionic liquids: Aqueous biphasic systems of water-miscible ionic liquids and water-structuring salts for recycle, metathesis, and separations. *J. Am. Chem. Soc.* **2003**, *125*, 6632−6633.

(7) Bhattacharjee, A.; Varanda, C.; Freire, M. G.; Matted, S.; Santos, L.M.N.B.F.; Marrucho, I. M.; Coutinho, J. A. P. Density and viscosity data for binary mixtures of 1-alkyl-3-methylimidazolium alkylsulfates + water. *J. Chem. Eng. Data* **2012**, *57*, 3473−3482.

(8) Wang, J.-Y.; Zhao, F.-Y.; Liu, Y.-M.; Wang, X.-L.; Hu, Y.-Q. Thermophysical properties of pure 1-ethyl-3-methylimidazolium methylsulphate and its binary mixtures with alcohols. *Fluid Phase Equilib.* **2011**, *305*, 114−120.

(9) Sánchez, L. G.; Espel, J. R.; Onink, F.; Meindersma, G. W.; Haan, A.B.d. Density, viscosity, and surface tension of synthesis grade imidazolium, pyridinium, and pyrrolidinium based room temperature ionic liquids. *J. Chem. Eng. Data* **2009**, *54*, 2803−2812.

(10) Tariq, M.; Forte, P. A. S.; Gomes, M. F. C.; Lopes, J. N. C.; Rebelo, L. P. N. Densities and refractive indices of imidazolium- and phosphonium-based ionic liquids: Effect of temperature, alkyl chain length, and anion. *J. Chem. Thermodyn.* **2009**, *41*, 790−798.

(11) Cláudio, A. F. M.; Freire, M. G.; Freire, C. S. R.; Silvestre, A. J. D.; Coutinho, J. A. P. Extraction of vanillin using ionic-liquid-based aqueous two-phase systems. *Sep. Purif. Technol.* **2010**, *75*, 39−47.

(12) Louros, C. L. S.; Cláudio, A. F. M.; Neves, C. M. S. S.; Freire, M. G.; Marrucho, I. M.; Pauly, J.; Coutinho, J. A. P. Extraction of biomolecules using phosphonium-based ionic liquids + $K_3PO_4$ aqueous biphasic systems. *Int. J. Mol. Sci.* **2010**, *11*, 1777−1791.

(13) Neves, C. M. S. S.; Freire, M. G.; Coutinho, J. A. P. Improved recovery of ionic liquids from contaminated aqueous streams using aluminium-based salts. *RSC Adv.* **2012**, *2*, 10882−10890.

(14) Freire, M. G.; Louros, C. L. S.; Rebelo, L. P. N.; Coutinho, J. A. P. Aqueous biphasic systems composed of a water-stable ionic liquid + carbohydrates and their applications. *Green Chem.* **2011**, *13*, 1536−1545.

(15) Zafarani-Moattar, M. T.; Hamzehzadeh, S. Phase diagrams for the aqueous two-phase ternary system containing the ionic liquid 1-butyl-3-methylimidazolium bromide and tri-potassium citrate at $T$ = (278.15, 298.15, and 318.15) K. *J. Chem. Eng. Data* **2009**, *54*, 833−841.

(16) Zafarani-Moattar, M. T.; Hamzehzadeh, S. Effect of pH on the phase separation in the ternary aqueous system containing the hydrophilic ionic liquid 1-butyl-3-methylimidazolium bromide and the kosmotropic salt potassium citrate at $T$ = 298.15 K. *Fluid Phase Equilib.* **2011**, *304*, 110−120.

(17) Han, J.; Wang, Y.; Li, Y.; Yu, C.; Yan, Y. Equilibrium phase behavior of aqueous two-phase systems containing 1-alkyl-3-methylimidazolium tetrafluoroborate and ammonium tartrate at different temperatures: Experimental determination and correlation. *J. Chem. Eng. Data* **2011**, *56*, 3679−3687.

(18) Han, J.; Yu, C.; Wang, Y.; Xie, X.; Yan, Y.; Yin, G.; Guan, W. Liquid−liquid equilibria of ionic liquid 1-butyl-3-methylimidazolium tetrafluoroborate and sodium citrate/tartrate/acetate aqueous two-phase systems at 298.15 K: Experiment and correlation. *Fluid Phase Equilib.* **2010**, *295*, 98−103.

(19) Han, J.; Wang, Y.; Yu, C.; Yan, Y.; Xie, X. Extraction and determination of chloramphenicol in feed water, milk, and honey samples using an ionic liquid/sodium citrate aqueous two-phase system coupled with high-performance liquid chromatography. *Anal. Bioanal. Chem.* **2011**, *399*, 1295−1304.

(20) Kurnia, K. A.; Freire, M. G.; Coutinho, J. A. P. Effect of polyvalent ions in the formation of ionic-liquid-based aqueous biphasic systems. *J. Phys. Chem. B* **2013**, *118*, 297−308.
(21) Shahriari, S.; Neves, C. M. S. S.; Freire, M. G.; Coutinho, J. A. P. Role of the Hofmeister series in the formation of ionic-liquid-based aqueous biphasic systems. *J. Phys. Chem. B* **2012**, *116*, 7252−7258.
(22) Passos, H.; Ferreira, A. R.; Cláudio, A. F. M.; Coutinho, J. A. P.; Freire, M. G. Characterization of aqueous biphasic systems composed of ionic liquids and a citrate-based biodegradable salt. *Biochem. Eng. J.* **2012**, *67*, 68−76.
(23) Freire, M. G.; Neves, C. M. S. S.; Marrucho, I. M.; Coutinho, J.o.A.P.; Fernandes, A. M. Hydrolysis of tetrafluoroborate and hexafluorophosphate counter ions in imidazolium-based ionic liquids. *J. Phys. Chem. A* **2009**, *114*, 3744−3749.
(24) Othmer, D. F.; Tobias, P. E. Liquid−liquid extraction data—The line correlation. *Ind. Eng. Chem.* **1942**, *34*, 693−696.
(25) González-Tello, P.; Camacho, F.; Blázquez, G.; Alarcón, F. J. Liquid−liquid equilibrium in the system poly(ethylene glycol) + $MgSO_4$ + $H_2O$ at 298 K. *J. Chem. Eng. Data* **1996**, *41*, 1333−1336.
(26) Mourão, T.; Cláudio, A. F. M.; Boal-Palheiros, I.; Freire, M. G.; Coutinho, J. A. P. Evaluation of the impact of phosphate salts on the formation of ionic-liquid-based aqueous biphasic systems. *J. Chem. Thermodyn.* **2012**, *54*, 398−405.
(27) Merchuk, J. C.; Andrews, B. A.; Asenjo, J. A. Aqueous two-phase systems for protein separation studies on phase inversion. *J. Chromatogr. B* **1998**, *711*, 285−293.
(28) Alvarez-Guerra, E.; Ventura, S. P. M.; Coutinho, J. A. P.; Irabien, A. Ionic liquid-based three phase partitioning (ILTPP) systems: Ionic liquid recovery and recycling. *Fluid. Phase Equilibr.* **2014**, *371*, 67−74.
(29) Gustafsson, J. *Visual MINTEQ—A Free Equilibrium Speciation Model*; KTH: Sweden, 2006; http://www.lwr.kth.se/English/OurSoftware/vminteq/.
(30) Neves, C. M. S. S.; Kurnia, K. A.; Coutinho, J. A. P.; Marrucho, I. M.; Lopes, J. N. C.; Freire, M. G.; Rebelo, L. P. N. Systematic study of the thermophysical properties of imidazolium-based ionic liquids with cyano-functionalized anions. *J. Phys. Chem. B* **2013**, *117*, 10271−10283.
(31) Cláudio, A. F. M.; Swift, L.; Hallett, J. P.; Welton, T.; Coutinho, J. A. P.; Freire, M. G. Extended scale for the hydrogen-bond basicity of ionic liquids. *Phys. Chem. Chem. Phys.* **2014**, *16*, 6593−6601.
(32) Tokuda, H.; Hayamizu, K.; Ishii, K.; Susan, M. A. B. H.; Watanabe, M. Physicochemical properties and structures of room temperature ionic liquids. 1. Variation of anionic species. *J. Phys. Chem. B* **2004**, *108*, 16593−16600.
(33) Cláudio, A. F. M.; Ferreira, A. M.; Shahriari, S.; Freire, M. G.; Coutinho, J.o.A.P. Critical assessment of the formation of ionic-liquid-based aqueous two-phase systems in acidic media. *J. Phys. Chem. B* **2011**, *115*, 11145−11153.
(34) Freire, M. G.; Carvalho, P. J.; Silva, A. M. S.; Santos, L.M.N.B.F.; Rebelo, L. P. N.; Marrucho, I. M.; Coutinho, J. A. P. Ion specific effects on the mutual solubilities of water and hydrophobic ionic liquids. *J. Phys. Chem. B* **2009**, *113*, 202−211.
(35) Ficke, L. E.; Brennecke, J. F. Interactions of ionic liquids and water. *J. Phys. Chem. B* **2010**, *114*, 10496−10501.
(36) Cha, S.; Ao, M.; Sung, W.; Moon, B.; Ahlstrom, B.; Johansson, P.; Ouchi, Y.; Kim, D. Structures of ionic liquid−water mixtures investigated by IR and NMR spectroscopy. *Phys. Chem. Chem. Phys.* **2014**, *16*, 9591−9601.
(37) Archer, D. W.; Monk, C. B. Ion-association constants of some acetates by pH (glass electrode) measurements. *J. Chem. Soc.* **1964**, 3117−3122.
(38) Ventura, S. P. M.; Neves, C. M. S. S.; Freire, M. G.; Marrucho, I. M.; Oliveira, J.; Coutinho, J. A. P. Evaluation of anion influence on the formation and extraction capacity of ionic-liquid-based aqueous biphasic systems. *J. Phys. Chem. B* **2009**, *113*, 9304−9310.
(39) Hofmeister, F. Zur Lehre von der Wirkung der Salze. *Archiv. Exp. Pathol. Pharm.* **1888**, *24*, 247−260.
(40) Daniele, P. G.; De Robertis, A.; De Stefano, C.; Sammartano, S.; Rigano, C. On the possibility of determining the thermodynamic parameters for the formation of weak complexes using a simple model for the dependence on ionic strength of activity coefficients: $Na^+$, $K^+$, and $Ca^{2+}$ complexes of low molecular weight ligands in aqueous solution. *J. Chem. Soc., Dalton Trans.* **1985**, 2353−2361.
(41) Oscarson, J. L.; Gillespie, S. E.; Christensen, J. J.; Izatt, R. M.; Brown, P. R. Thermodynamic quantities for the interaction of $H^+$ and $Na^+$ with $C_2H_3O^{2-}$ and $Cl^-$ in aqueous solution from 275 to 320 °C. *J. Solution Chem.* **1988**, *17*, 865−885.
(42) Fournier, P.; Oelkers, E. H.; Gout, R.; Pokrovski, G. Experimental determination of aqueous sodium-acetate dissociation constants at temperatures from 20 to 240 °C. *Chem. Geol.* **1998**, *151*, 69−84.
(43) van Rantwijk, F.; Sheldon, R. A. Biocatalysis in ionic liquids. *Chem. Rev.* **2007**, *107*, 2757−2785.
(44) Mei, L.-H.; Lin, D.-Q.; Zhu, Z.-Q.; Han, Z.-X. Densities and viscosities of polyethylene glycol + salt + water systems at 20 °C. *J. Chem. Eng. Data* **1995**, *40*, 1168−1171.
(45) Regupathi, I.; Govindarajan, R.; Pandian Amaresh, S.; Murugesan, T. Densities and viscosities of polyethylene glycol 6000 + triammonium citrate + water systems. *J. Chem. Eng. Data* **2009**, *54*, 3291−3295.


DOI: 10.1021/je501044u
*J. Chem. Eng. Data* 2015, 60, 1674−1682